Desalination and Water Treatment
www.deswater.com
doi: 10.5004/dwt.2023.29181

282 (2023) 53–69
January

RETRACTED

Thermal analysis of water distillation system using PV/T collector combined single basin still

Viet Van Hoang[a,b,c], Bao The Nguyen[a,b,*], Huy Dang Ho[a,b]

[a]*Department of Heat and Refrigeration Engineering, Ho Chi Minh City University of Technology (HCMUT), 268 Ly Thuong Kiet Street, District 10, Ho Chi Minh City, Vietnam, Tel.: +84-906331133; email: thebao@hcmut.edu.vn (B.T. Nguyen), Tel.: +84-937911988; email: hoangvanviet@lttc.edu.vn (V.V. Hoang), Tel.: +84-9396261696; email: huy.hodang@hcmut.edu.vn (H.D. Ho)*
[b]*Vietnam National University Ho Chi Minh City, Linh Trung Ward, Thu Duc District, Ho Chi Minh City, Vietnam*
[c]*Ly Tu Trong College of Ho Chi Minh City, 390 Hoang Van Thu street, Ward 4, Tan Binh District, Ho Chi Minh City, Vietnam*

Received 2 August 2022; Accepted 3 December 2022

ABSTRACT

This paper introduces a novel photovoltaic thermal (PV/T) system, in which the water used to cool solar cells (PV cells) is used to provide hot water at night for a solar passive single basin still – a distillation device with simple design and operation. This proposed PV/T system helps the solar still produce distilled water at both day and night, hence increasing the distilled yield in comparison with that of conventional solar still. The article also presents a simulation program written in MATLAB based on the thermal analysis equations of PV/T system equipment, thereby calculating the parameters of the equipment as well as the power output and distilled water of the whole PV/T system. The comparison of the calculated results and the experimental results shows that the written simulation program has high accuracy and reliability. The errors between experimental and simulation results are around 4.24%–7.11%. Then, the simulation program is used to calculate the optimal volume of water in the tank and thereby predicts the production of distilled water at typical days of 6 months from January to June. The simulation results show that the use of hot water from PV/T collector to distil water at night increases the output of distilled water from 35.2% to 41.7% compared to that of traditional solar single basin stills.

Keywords: PV/T collector; Cooling PV systems; Efficiency of PV system; Solar single basin still; Nocturnal distillation

1. Introduction

Fossil fuel reserves are increasingly depleted and this requires people to find alternative energy sources to meet actual needs when the world population is increasing. Humans take advantage of mining to generate electricity and heat, but applications that can be applied to simultaneously exploit electrical and thermal energy sources have not been fully utilized. There are many abundant and inexhaustible energy sources such as solar energy, wind energy, wave energy, etc. In these mentioned sources of renewable energy, solar energy is stable and can be used almost everywhere. Solar photovoltaics (PV) systems are now preferred to be installed for direct electricity generation due to their compactness, ease of installation and flexible capacity range, suitable for small, medium and large purposes. Not only that, in some countries, the government also has preferential policies for the use of solar power.

On the other hand, people in the world are increasingly facing the lack of clean water for living nowadays. Every year, millions of people die from lack of clean water and from the diseases relating to drinking and living water. There is a lot of technology in the world to produce fresh

* Corresponding author.

1944-3994/1944-3986 © 2023 Desalination Publications. All rights reserved.

RETRACTED

water from sea water or brackish water. However, these technologies are mostly expensive, not suitable for the poor and developing countries and communities where most of the water shortages are occurring. In addition, most of industrial-scale distillation technologies and equipment consume a lot of energy, contributing to the depletion of fossil fuel energy sources and increasing environmental pollution. It is therefore necessary to promote cheap, less energy-efficient and environmentally friendly distillation methods. The methodology and technology of solar distillation almost meet these criteria: simple equipment with low cost, no use of fossil fuels and no contribution to the environmental pollution [1].

In fact, the photovoltaic conversion efficiency of commercial solar panels is only about 15%–20% depending on the PV type and working conditions, the rest of the energy is converted into heat and discharged into the environment. Solar cell efficiency decreases with increasing the operating temperature of PV cells. The temperature coefficient is shown in Table 1 for different PV cell types [2]. Moreover, the uneven temperature distribution in PV panels will increase the thermal stress inside the solar module. Therefore, in order to limit the efficiency loss of solar PV cells as much as possible and increase the life of solar cells, researchers have proposed many methods of cooling solar cells by creating systems called photovoltaics/thermal (PV/T) systems. PV/T systems are known as co-generation of heat and electricity because in addition to the ability to generate electricity, the excess heat removed from solar cells also has great potential for drying, water or space heating and water distillation.

There have been many studies in the world on cooling solar PV panels to increase their efficiencies. Akbarzadeh and Wadowski [3] designed a water-cooled PV system incorporating a heat pipe and found that the output power of the solar cells increased by almost 50%. Chaniotakis [4] designed a water-cooled PV system and an air-cooled system and concluded that water-cooled systems increase efficiency more than air-cooled systems. Batoul [5] investigated the effect of airflow on the performance of PV panels using computational fluid dynamics (CFD) and found that the shape and conformation of the PV system had a large impact to the efficiency of the cooled panels. Tonui and Tripanagnostopoulos [6] designed a PV system cooled by forced or natural convection air. Ho et al. [7] studied the cooling system for solar cells and found that the power output of cooled solar cells increased by 27.35% compared with that of uncooled cells. However, the combination of cooling systems for PVs to distill water is currently very rare. Hedayati et al. [8] presented a PV/T system using a stepped cascade solar still and reported that the volume of distilled water was increased by about 20%. However, this type must consume electricity to run the pump to supply the distillation equipment.

Table 1
Temperature coefficient of solar cells [2]

PV Type	Efficiency of commercial PV (%)	Efficiency decreases when temperature increases (%/°C)
Mono c-Si	15–20	–0.446
Poly c-Si	10–14	–0.387
a-Si	5–9	–0.234
CdTe	7	–0.172

This paper introduces a new idea of PV/T system, in which the water used to cool solar cells (PV cells) is used to provide hot water at night for a solar passive single basin still – a distillation device with simple design and operation. Therefore, this solar still can produce distilled water at both day and night, hence increasing the distilled yield from 35.2% to 41.7% compared to that of conventional solar still which only works during day time. The article also presents a simulation program written in MATLAB based on the thermal analysis equations of PV/T system equipment, thereby calculating the parameters of the equipment as well as the power output and distilled water of the whole PV/T system. The comparison of the calculated results and the experimental results shows that the written simulation program has high accuracy and reliability. Then, the simulation program is used to recommend the optimal volume of water in the tank and thereby predict the production of distilled water at typical days of 6 months from January to June.

2. Operation principle of the system and the experimental model

The water distillation system using a PV/T collector combined with a solar passive single basin still is presented in Fig. 1. During the day, the PV/T system receives solar radiation and converts it into electricity and heat. Part of the power of the DC current is converted into AC current by the inverter to supply only the pump motor, the rest will be sent to the consumers. The heat energy is absorbed by two zigzag tube type heat exchangers and transferred to pure water flowing inside the tube. Pure water after receiving heat with temperature t_{fo} is brought to a coil tube heat exchanger to release heat to seawater in the tank, then reduced to temperature t_{fi} and continued to be pumped to collector PV/T for reheating. The amount of seawater stored in the tank will be heated until the solar radiation is stopped. On the one hand, inside the single basin still, seawater receives solar radiation to evaporate and condense continuously until the seawater temperature is equal to the ambient temperature and is discharged outside. At night, the seawater inside the high temperature tank will naturally flow down to the basin to carry out the process of evaporation, condensing to create distilled water. Due to distillation at night, the ambient temperature is reduced, so the distillation capacity is improved. As a result, the total amount of distilled water during the day and night is significantly increased compared to the traditional solar stills only operating during the time when the solar radiation is available.

Fig. 2 presents an overview of as well as some of the main equipment in the experimental PV/T model.

3. Mathematical model

The simulation program is set up by the energy balance equations at the components of the PV/T system and the

RETRACTED

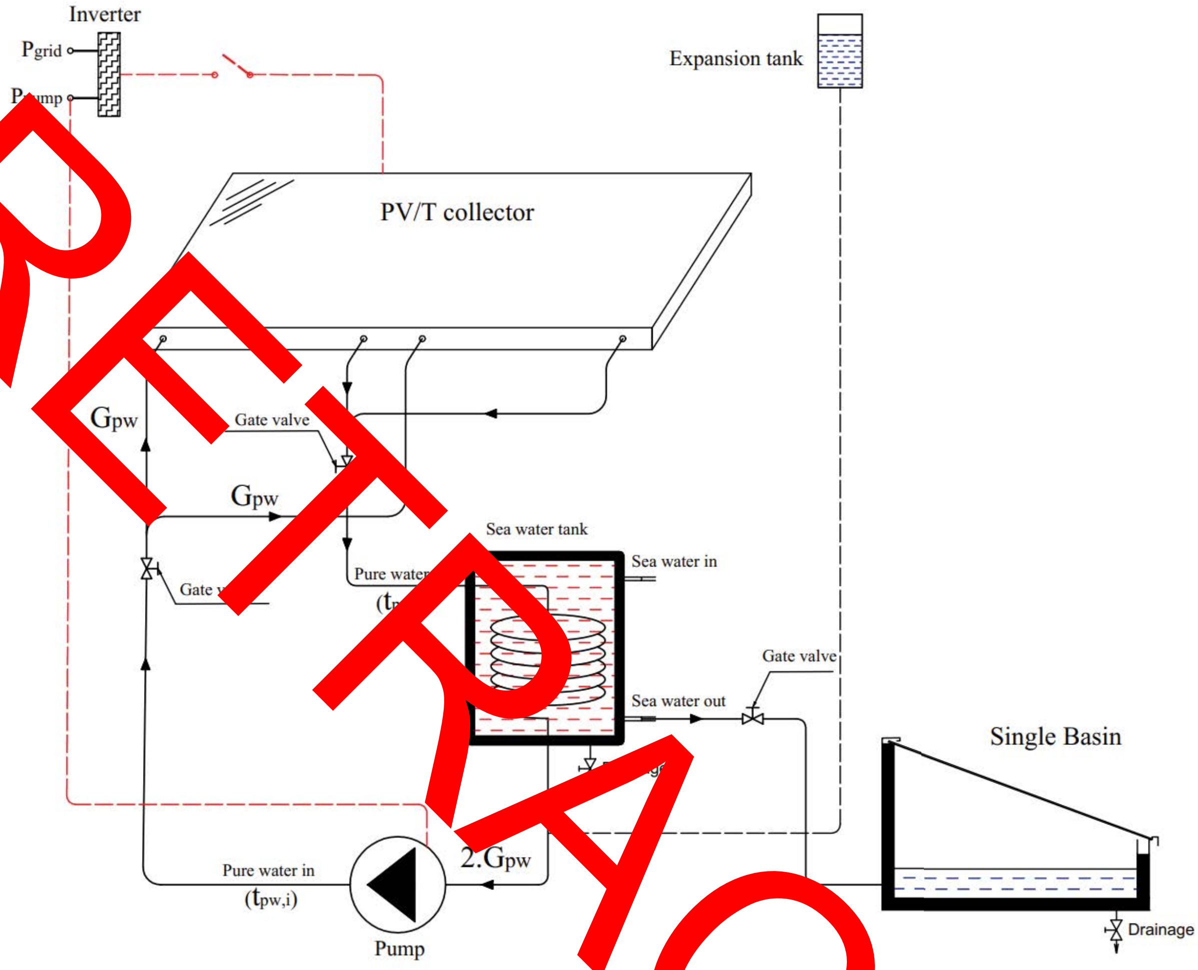

Fig. 1. Water distillation system using PV/T collector combined with single basin still.

single basin still. All equations are written on the basis of the following assumptions:

- Ignore the heat flow from the outside to the 4 sides of the PV/T system and the single basin still;
- Physical parameters at glass cover, PV layer, absorption plate, copper tube, insulation layer of PV/T collector and at glass cover, absorption plate of still are unchanged;
- Thermophysical parameters of pure water at PV/T collector and seawater at distillation system change with temperature;
- Constant flow of pure water according to the length of the heat exchanger tube of PV/T collector;
- The temperature of the glass cover, PV layer, absorbing plate, copper tube, purified water and insulation layer in PV/T collector and of the glass cover, seawater, absorbent plate of still changes with time.
- The temperature of the seawater in the container is uniform;
- Pump pressure loss includes valve loss, 1 pass loss through PV/T collector heat exchanger tube and coil loss inside the seawater tank.
- Area of glass cover, PV layer, absorption plate and insulation layer are equal and are equal to PV/T collector area ($A_g = A_{pvl} = A_{ab} =$ [illegible] $= A_{PV/T}$)

The energy balance equations at the components of the PV/T collector, seawater tank and still are written as follows:

3.1. PV/T collector

3.1.1. Glass

$$\delta_g \rho_g c_{p,g} \frac{dT_g}{d\tau} = h_{c-a,g}\left(T_a - T_g\right) + h_{r-a,g}\left(T_{sky} - T_g\right) + h_{g,pvl}\left(T_{pvl} - T_g\right) + \alpha_g I_s \quad (1)$$

where I_s, T_a, v_s is the average value over a period of solar radiation intensity, ambient temperature and average wind speed respectively;

Heat transfer coefficient by convection and radiation between coated glass and atmosphere [1].

$$h_{c-a,g} = h_{c-a,ins} = 2.8 + 3v_a \left(\frac{W}{m^2K}\right) \quad (2)$$

RETRACTED

Fig. 2. The overview layout and some of the main equipment in the experimental PV/T model. (a) Overall layout of equipment of experimental PV/T system, (b) solar panels and installation location of temperature sensors, (c) water distillation device seen from above and locations of glass temperature measured sensors, (d) sea water tank seen from inside, and (e) sea water tank seen from outside.

RETRACTED

$$h_{r-\text{sky},g} = \varepsilon_g \sigma \left[\left(T_{\text{sky}}\right)^2 + \left(T_g\right)^2 \right] \left(T_{\text{sky}} + T_g\right) \left(\frac{W}{\text{m}^2 K}\right) \tag{3}$$

Sky temperature is calculated as [9]:

$$T_{\text{sky}} = 0.0522\left(T_a\right)^{1.5} \tag{4}$$

Heat transfer coefficient by thermal conductivity between the glass cover and PV layer:

$$h_{g,\text{pvl}} = \frac{1}{\delta_g / k_g} \left(\frac{W}{\text{m}^2 K}\right) \tag{5}$$

3.1.2. PV layer

$$\delta_{\text{pvl}} \rho_{\text{pvl}} c_{p,\text{pvl}} \frac{dT_{\text{pvl}}}{d\tau} = \left(\tau_g \alpha_{\text{pvl}}\right) I_S + h_{\text{pvl},ab} \left(T_{ab} - T_{\text{pvl}}\right) - fE_{\text{elec}} + h_{g,\text{pvl}} \left(T_g - T_{\text{pvl}}\right) \tag{6}$$

where the specific electrical capacity of the PV layer:

$$E_{\text{elec}} = I_S \eta_r \left[1 - B_r \left(T_{\text{pvl}} - T_r\right) \right] \left(\frac{W}{\text{m}^2}\right) \tag{7}$$

Packing factor:

$$f = \frac{A_{\text{pvc}}}{A_{PV/T}} \tag{8}$$

Heat transfer coefficient by thermal conduction between PV layer and absorption plate:

$$h_{\text{pvl},ab} = \frac{1}{\delta_{\text{ad}} / k_{\text{ad}}} \left(\frac{W}{m^2 K}\right) \tag{9}$$

3.1.3. Absorber

$$\delta_{ab} \rho_{ab} c_{p,ab} \frac{dT_{ab}}{d\tau} = h_{\text{pvl},ab} \left(T_{\text{pvl}} - T_{ab}\right) + \frac{2A_{t,ab}}{A_{ab}} h_{ab,t} \left(T_t - T_{ab}\right) + \left(1 - \frac{2A_{t,ab}}{A_{ab}}\right) h_{ab,\text{ins}} \left(T_{\text{ins}} - T_{ab}\right) \tag{10}$$

T in which heat transfer coefficient between absorber plate and tube:

$$h_{ab,t} = \frac{1}{\frac{\delta_{ab}}{k_{ab}} + \frac{\delta_t}{k_t}} \left(\frac{W}{\text{m}^2 K}\right) \tag{11}$$

Heat transfer coefficient by heat conduction between the absorption plate and the insulation:

$$h_{ab,\text{ins}} = \frac{1}{\delta_{\text{ins}} / k_{\text{ins}}} \left(\frac{W}{\text{m}^2 K}\right) \tag{12}$$

The contact area between tube and absorption plate is given [10]:

$$A_{t,ab} = \delta_{ab} L_t \left(\text{m}^2\right) \tag{13}$$

3.1.4. Tube

$$L_t A_t \rho_t C_{p,t} \frac{dT_t}{d\tau} = A_{t,ab} h_{ab,t} \left(T_{ab} - T_t\right) + \text{Pe}_i L_t h_{\text{pw},t} \left(T_f - T_t\right) + A_{t,ins} h_{t,ins} \left(T_{\text{ins}} - T_t\right) \tag{14}$$

In which:

- The cross-sectional area of the tube (m^2): $A_t = \frac{\pi}{4}\left(D_{t,0}^2 - D_{t,i}^2\right)$ (15)
- $D_{t,o}$ is the outer diameter of tube (m); $D_{t,i}$ is the outer diameter of tube (m)
- Inner circumference of tube (m): $\text{Pe}_i = \pi D_{t,i}$ (16)
- Inner circumference of tube (m): $\text{Pe}_0 = \pi D_{t,0}$ (17)
- The contact area of the tube and the insulation (m^2): $A_{t,\text{ins}} = L_t \text{Pe}_0 - A_{t,ab}$ (18)

L_t is the length of 1 tube pass in the PV/T collector (m)

Heat transfer coefficient by heat conduction between tube and insulation:

$$h_{t,\text{ins}} = h_{\text{ins},ab} = \frac{1}{\delta_{\text{ins}} / k_{\text{ins}}} \left(\frac{W}{m^2 K}\right) \tag{19}$$

Heat transfer coefficient by convection of water and tube [5]:

$$h_{\text{pw},t} = \frac{\text{Nu}_{\text{pw}} k_{\text{pw}}}{D_{t,i}} \left(\frac{W}{m^2 K}\right) \tag{20}$$

Prandlt value [5]:

$$\text{Pr}_{\text{pw}} = \frac{\mu_{\text{pw}} c_{p,pw}}{k_{\text{pw}}} \tag{21}$$

The water velocity in 1 tube pass:

$$\omega_{\text{pwl}} = \frac{4G_{\text{pw}}}{\rho_{\text{pw}} \pi D_{t,i}} \left(m / s\right) \tag{22}$$

Reynold value:

$$\text{Re}_{\text{pw}} = \frac{\rho_{\text{pw}} \omega_{\text{pwl}} D_{t,i}}{\mu_{\text{pw}}} \tag{23}$$

- Nusselt value is dependent in Reynold number as follows [11]:

RETRACTED

+With $\text{Re}_{\text{pw}} < 2300: \ \text{Nu}_{\text{pw}} = 4.364$ (24)

+With $\text{Re}_{\text{pw}} > 2300: \ \text{Nu}_{\text{pw}} = 0.023\left(\text{Re}_{\text{pw}}\right)^{0,8}\left(\text{Pr}_{\text{pw}}\right)^{0,4}$ (25)

The thermophysical parameters of pure water and seawater are calculated according to Table 2.

3.1.5. Pure water

$$L_t A_{\text{pw}} \rho_{\text{pw}} c_{p,\text{pw}} \frac{dT_{\text{pw}}}{d\tau} = \text{Pe}_i L_t h_{\text{pw},t}\left(T_t - T_{\text{pw}}\right) - G_{\text{pw}} c_{p,\text{pw}}\left(T_{\text{pw},0} - T_{\text{pw},i}\right) \quad (26)$$

In which:

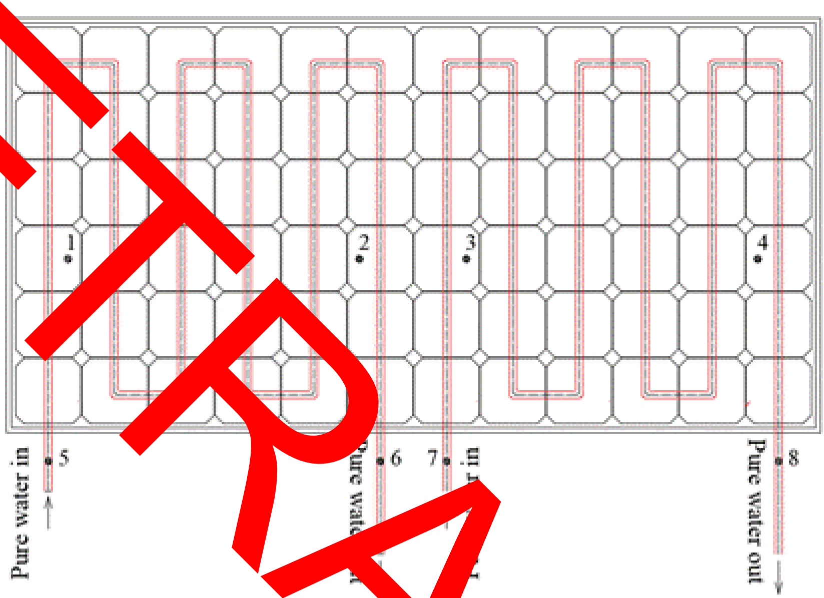

Fig. 3. Layout diagram of the zigzag-tube type heat exchanger inside PV/T and the positions of temperature measured sensors.

Table 2
Physical properties of water [4]

Physical properties of water	Note
$\rho = \rho_c\left(\begin{matrix}1 + b_1\psi^{1/3} + b_2\psi^{2/3} + b_3\psi^{5/3} \\ +b_4\psi^{16/3} + b_5\psi^{43/3} + b_6\psi^{110/3}\end{matrix}\right)(\text{kg/m}^3)$ $\psi = 1 - T/T_c;\ T_c = 647.096\ [K];\ \rho_c = 332\ (\text{kg/m}^3)$	b_1 = 1.99274064; b_2 = 1.09965342; b_3 = –0.510839303; b_4 = –1.75493479; b_5 = –45.5170352; b_6 = –6.74694450 × 10^5.
$c_p = a + b(T-273.15) + c(T-273.15)^{1.5} + d(T-273.15)^2 + e(T-273.15)^{2.5}\ (kJ/\text{kg K})$	a = 4.2174356; b = –0.0056181625; c = 0.0012992528; d = –0.00011535353; e = 4.14964 × 10^–6.
$\mu = \frac{1}{a + b(T-273.15) + c(T-273.15)^2 + d(T-273.15)^3}\left(\frac{\text{kg}}{\text{ms}}\right)$	a = 557.82468; b = 19.408782; c = 0.1360459; d = –3.1160832 × 10^–4.
$k = a + b(T-273.15) + c(T-273.15)^{1.5} + d(T-273.15)^2 + e(T-273.15)^{0.5}\ (W/\text{mK})$	a = 0.5650285; b = 0.0026363895; c = –0.00012516934; d = –1.5154918 × 10–6; e = –0.0009412945.

RETRACTED

- Cross-sectional area of water flowing in 1 pipe pass (m²)

$$A_{pw} = \frac{\pi D_{t,i}^2}{4} \quad (27)$$

[illegible]et:

$$T_{pw} = \frac{T_{pw,i} + T_{pw,o}}{2} \Rightarrow T_{pw,o} = 2T_{pw} - T_{pw,i}$$

Eq. (26) becomes:

$$L_t A_{pw} \rho_{pw} c_{p,pw} \frac{dT_{pw}}{d\tau} = \text{Pe}_i L_t h_{pw,t} \left(T_t - T_{pw}\right) - 2G_{pw} c_{p,pw} \left(T_{pw} - T_{pw,i}\right) \quad (28)$$

3.1.6. Insulation

$$\delta_{ins} \rho_{ins} c_{p,ins} \frac{dT_{ins}}{d\tau} = \left(1 - \frac{2A_{t,ab}}{A_{ins}}\right) h_{ins,ab} \left(T_{ab} - T_{ins}\right) + \frac{2A_{t,ins}}{A_{ins}} h_{t,ins} \left(T_t - T_{ins}\right) + h_{c-a,ins} \left(T_a - T_{ins}\right) \quad (29)$$

3.2. Seawater tank

$$Q_{hw} = V_{hw} \rho_{hw} c_{p,hw} \frac{dT_{hw}}{d\tau} = Q_{c1} - h_{hw1,a} \left(T_{hw} - T_a\right) - 2A_n h_{hw2,a} \left(T_{hw} - T_a\right) (W) \quad (30)$$

where Q_{hw}: heat that sea water receives (W); V_{hw}: volume of water in the tank (m³); $c_{p,hw}$: specific heat of seawater (J/kg·K)

The heat of pure water released at the spiral coil is calculated by one of the following two equations:

$$Q_{c1} = 2G_{pw} c_{p,pw} \left(T_{pw,0} - T_{pw,i}\right) (W) \quad (31)$$

Or: $Q_{c2} = F_{coil} h_{pw,t} \left(T_{pw} - T_s\right) (W)$ (32)

where T_{pw} and T_s are the average temperature of pure water in the spiral coil and the wall temperature, respectively.

Give $T_s = \frac{T_{pw} + T_{hw}}{2} [K]$ (33)

- Area of heat exchange between pure hot water inside the spiral coil and sea water in the tank.

$$F_{coil} = \pi D_{c,i} L_c \left(m^2\right) \quad (34)$$

+ $D_{c,i} = D_{t,i}$: Inner diameter of spiral coil (m)
+ L_c: Length of the spiral coil (m)

- The velocity of water in spiral coil: $\omega_{pw2} = 2\omega_{pw1} (m/s)$ (35)
- Reynold, Nusselt values and the heat transfer coefficient by convection of pure water in the spiral coil is similar

Table 3
Design and operation parameters of the PV/T collector and single basin solar still

Components	Parameters	Value	Unit
PV/T collector	$A_{PV/T}$	2	m²
Glass	δ_g	0.004	m
	ρ_g	2,200	kg/m³
	$c_{p,g}$	670	J/kg·K
	k_g	0.9	W/m·K
	ε_g	0.88	
	α_g	0.04	
	τ_g	0.93	
	f	0.9	
PV layer	δ_{pvl}	0.0011	m
	ρ_{pvl}	2,320	kg/m³
	$c_{p,pvl}$	900	J/kg·K
	k_{pvl}	140	W/m·K
	α_{pvl}	0.9	
	η_r	20	%
	B_r	0.00405	1/K
	I_r	1,000	W/m²
	T_r	298.15	K
Absorber	δ_{ab}	0.0002	m
	[illegible]	2,702	kg/m³
	[illegible]	896	J/kg·K
	k_{ab}	310	W/m·K
Tube	$D_{t,o}$	0.00952	m
	$D_{t,i}$	0.00792	m
	L_t	[illegible]	m
	ρ_t	8,900	kg/m³
	[illegible]	[illegible]	J/kg·K
	k_t	[illegible]	W/m·K
Insulation	δ_{ins}	0.03	m
	ρ_{ins}	[illegible]	kg/m³
	$c_{p,ins}$	670	J/kg·K
	k_{ins}	0.034	W/m·K
Sea water tank	L_c	15	m
	$D_{ins,i}$	[illegible]	m
	$\delta_{ins,hw}$	[illegible]	m
Single basin solar still	A_{sw}	1	m²
	A_g	1.13	m²
	A_b	1	m²
	ε_{sw}	0.95	
	α_{sw}	0.05	
	τ_{sw}	0.95	
	α_b	0.9	
	δ_b	0.001	m
	ρ_b	7900	kg/m³

to that of the water in the heat exchanger tube pass at PV/T collector.

Total heat transfer coefficient from hot water through the wall of the tank to the surrounding environment [12]:

$$h_{\text{hw1},a} = \frac{1}{\frac{1}{2\pi k_{\text{ins}}}\ln\left(\frac{D_{\text{ins},0}}{D_{\text{ins},i}}\right) + \frac{1}{\pi D_{\text{ins},0} H_{\text{hw}} h_{c-a,\text{ins}}}}\left(W/K\right) \quad (36)$$

The coefficient of total heat transfer from hot water through the top and bottom of the tank to the surrounding environment [12]:

$$h_{\text{hw}2,a} = \frac{1}{\frac{\delta_{\text{ins,hw}}}{k_{\text{ins}}} + \frac{1}{h_{c-a,\text{ins}}}}\left(W/m^2K\right) \quad (37)$$

With $\delta_{\text{ins,hw}}$, k_{ins} is the thickness and thermal conductivity of the seawater tank insulation

+ $D_{\text{ins},i}$: Inner diameter of hot water tank insulation (m)
+ Outer diameter of hot water tank insulation (m)

$$D_{\text{ins},0} = D_{\text{ins},i} + 2\delta_{\text{ins,hw}} \quad (38)$$

+ Height of water inside the tank (m)

$$H_{\text{hw}} = \frac{V_{\text{hw}}}{A_n} \quad (39)$$

+ Area of the top or the bottom of the tank (m^2)

$$A_n = \frac{\pi D_{\text{hw}}^2}{4} \quad (40)$$

+ D_{hw}: diameter of water in the tank (m) (give $D_{\text{hw}} = D_{\text{ins},i}$)
+ $H_{\text{ins}} = H_{\text{hw}}$: height of the tank insulation (m)

3.3. Single basin still

The coefficient of heat transfer by radiation and convection between the glass cover and the environment $h_{c-a,g}$, $h_{r-\text{sky},g}$ is calculated in the same way as the PV/T collector.

The partial pressure of water vapor in the glass cover and sea water is given in [8]:

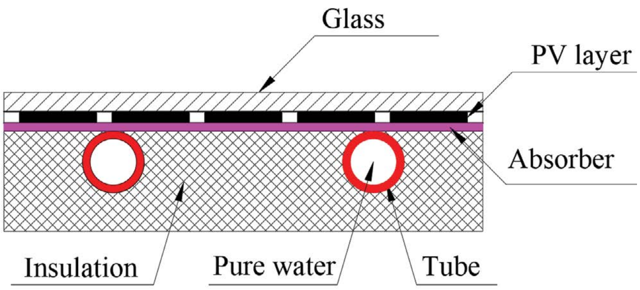

Fig. 4. Cross-section of PV/T collector.

$$P_g = \exp\left[25.317 - \left(\frac{5144}{T_g}\right)\right]\left(N/m^2\right) \quad (41)$$

$$P_{\text{sw}} = \exp\left[25.317 - \left(\frac{5144}{T_{\text{sw}}}\right)\right]\left(N/m^2\right) \quad (42)$$

Heat transfer coefficient by convection between the sea water and the glass cover according to [1]:

$$h_{c-\text{sw},g} = 0.884\left[\left(T_{\text{sw}} - T_g\right) + \frac{\left(p_{\text{sw}} - p_g\right)\left(T_{\text{sw}}\right)}{268.9\times 10^3 - p_{\text{sw}}}\right]^{1/3}\left(\frac{W}{m^2K}\right) \quad (43)$$

Radiative heat transfer coefficient between the sea water and the glass cover [1]:

$$h_{r-\text{sw},g} = \varepsilon_{\text{eff}}\sigma\left[\frac{\left(T_{\text{sw}}\right)^4 - \left(T_g\right)^4}{T_{\text{sw}} - T_g}\right]\left(\frac{W}{m^2K}\right) \quad (44)$$

With:

$$\varepsilon_{\text{eff}} = \left[\frac{1}{\varepsilon_g} + \frac{1}{\varepsilon_{\text{sw}}} - 1\right]^{-1} \quad (45)$$

Heat transfer coefficient by evaporation between the seawater and the glass cover [1]:

$$h_{e-\text{sw},g} = 0.016273 h_{c-\text{sw},g}\frac{\left(p_{\text{sw}} - p_g\right)}{\left(T_{\text{sw}} - T_g\right)}\left(\frac{\text{W}}{m^2\,\text{K}}\right) \quad (46)$$

Total heat transfer coefficient between the sea water and the glass cover according to [1]:

$$h_{\text{sw},g} = h_{r-\text{sw},g} + h_{c-\text{sw},g} + h_{e-\text{sw},g}\left(\frac{W}{m^2K}\right) \quad (47)$$

Heat transfer coefficient between the basin liner and environment $h_{b,a}$.

Heat transfer coefficient between the basin liner and the sea water $h_{b,\text{sw}}$.

Distilled water yield [1]:

$$m_{\text{ev}} = \frac{A_{\text{sw}} h_{e-\text{sw},g}\left(T_{\text{sw}} - T_g\right)d\tau}{h_{\text{fg}}}(\text{kg}) \quad (48)$$

+ Vapor temperature

$$T_v = \frac{T_{\text{sw}} + T_g}{2}\left[K\right] \quad (49)$$

RETRACTED

RETRACTED

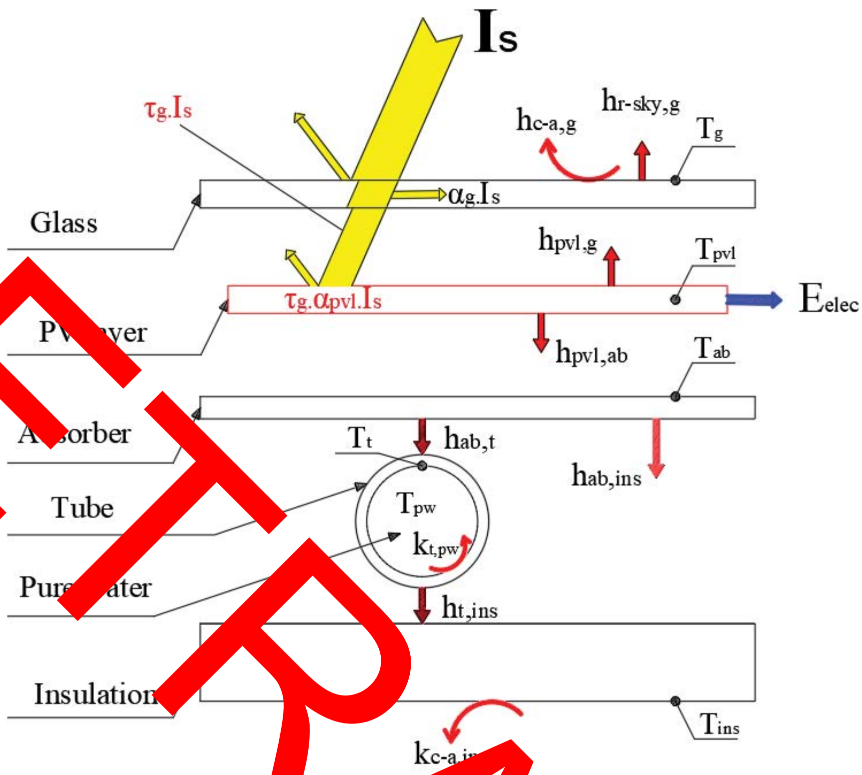

Fig. 5. Heat flow between PV/T collector components.

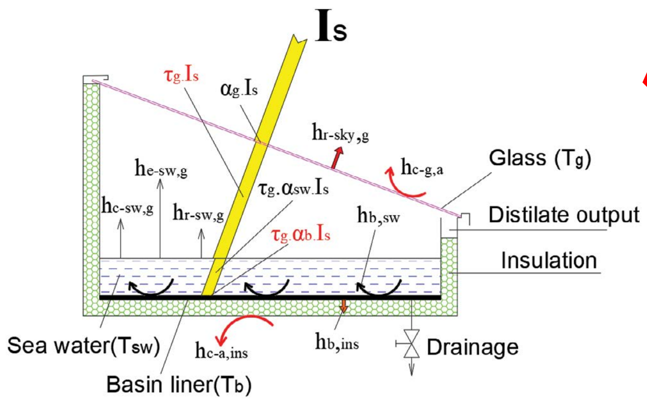

Fig. 6. Heat flow between components of single basin still.

- The latent heat of water vapor h_{fg} [8]:

  + If $T_v \leq 343.15$ [K]

$$h_{fg} = 2.4935\begin{bmatrix} 10^6 - 947.79\left(T_v - 273.15\right) \\ +0.13132\left(T_v - 273.15\right)^2 \\ -0.0047974\left(T_v - 273.15\right)^3 \end{bmatrix}\left(J/\text{kg}\right) \quad (50)$$

  + If $T_v > 343.15$ [K]

$$h_{fg} = 3.1615\left[10^6 - 761.6\left(T_v - 273.15\right)\right]\left(J/\text{kg}\right) \quad (51)$$

3.3.1. Heat balance equation at the glass cover

$$A_g\delta_g\rho_g c_{p,g}\frac{dT_g}{d\tau} = A_g h_{c-a,g}\left(T_a - T_g\right) + A_g h_{r-\text{sky},g}\left(T_{\text{sky}} - T_g\right) + A_{\text{sw}} h_{\text{sw},g}\left(T_{\text{sw}} - T_g\right) + A_g\alpha_g I_s \quad (52)$$

3.3.2. Heat balance equation at the seawater layer

$$A_{\text{sw}}\delta_{\text{sw}}\rho_{\text{sw}}c_{p,\text{sw}}\frac{dT_{\text{sw}}}{d\tau} = A_b h_{c-b,\text{sw}}(T_b - T_{\text{sw}}) + A_{\text{sw}}h_{\text{sw},g}(T_g - T_{\text{sw}}) + A_{\text{sw}}\tau_g\alpha_{\text{sw}}I_s \quad (53)$$

3.3.3. Heat balance equation at the basin liner

$$A_b\delta_b\rho_b c_{p,b}\frac{dT_b}{d\tau} = A_b h_{c-b,\text{sw}}\left(T_{\text{sw}} - T_b\right) + A_b h_{b,a}\left(T_a - T_b\right) + A_b\tau_g\tau_{\text{sw}}\alpha_b I_s \quad (54)$$

3.4. Energy values of seawater heating system using PV/T collector

Pump capacity:

$$P_{\text{pump}} = \frac{2G_{\text{pw}}\Delta p}{\eta_{\text{pump}}\rho_f}(W) \quad (55)$$

With η_{pump} = 0.8 is the electrical–mechanical efficiency of the pump

- Δp is the total pressure loss of the pump calculated according to [5] with the above-mentioned assumption.

Electricity that PV/T collector produces:

$$P_{elec0} = I_S A_{PV/T} \eta_{elec} \left(W\right) \quad (56)$$

Electricity after going through the inverter [13]:

$$P_{elec1} = \eta_{inv} P_{elec0} \left(W\right) \quad (57)$$

with η_{inv} = 0.[illegible] is the inverter efficiency [13]:

Electricity going to the grid:

$$P_{grid} = P_{elec1} - P_{pump} \left(W\right) \quad (58)$$

Energy efficiency of the PV/T system [13]:

$$\eta_{energy} = \frac{P_{grid} + Q_{hw}}{I_S A_{PV/T}} \quad (59)$$

4. Solution method

To simulate the entire system, the software MATLAB 2018b is chosen to perform, all steps are shown in the diagram in Fig. 7.

- Start the program
- Set design and operation parameters as Table 1

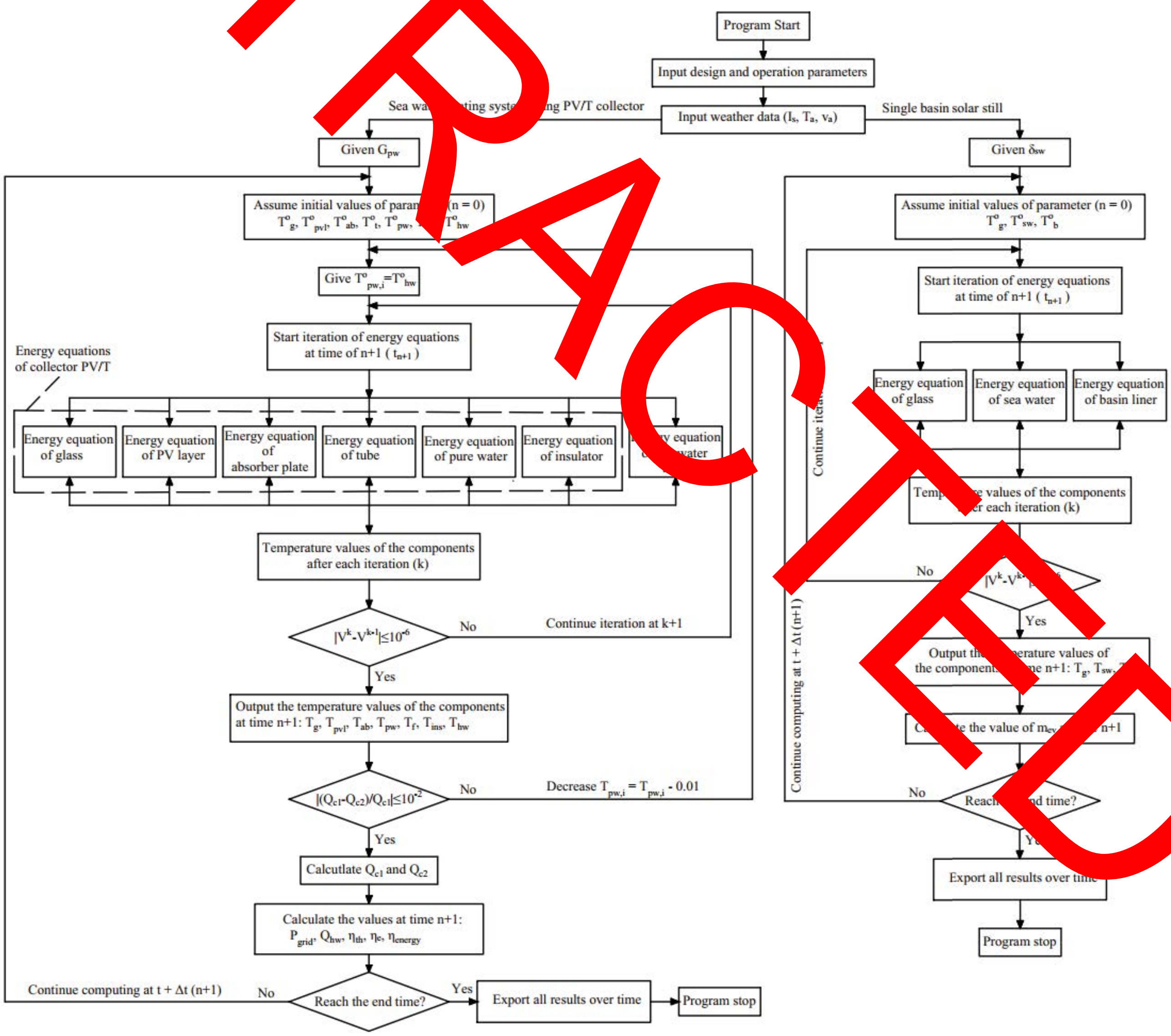

Fig. 7. Simulation diagram for PV/T system and single basin solar still.

RETRACTED

- Load weather data including solar radiation, ambient temperature and wind speed. Weather data values are actually measured and recorded every 5 min.

Thus, the simulation program is separated into 2 separate parts, Part 1 for seawater heating system using PV/T collector, Part 2 for single basin still.

To solve the unstable heat transfer differential equations in the components of the water heating system of PV/T collector to find the temperature over time of the glass cover (T_g), the PV layer (T_{pvl}), the absorption plate (T_{ab}), the heat exchange tube (T_t), purified water (T_{pw}), the insulation layer (T_{ins}) and the seawater in the tank (T_{hw}); as well as those of the single basin still to find temperature over time of the glass cover (T_g), seawater (T_{sw}), the basin liner (T_b), the numerical method in heat transfer is used. The unstable heat transfer differential equations will be discrete in time with the latent type finite difference method. In which the selected time step is Δt = 300 s (5 min) to match the experimental measurement time between two values of solar radiation intensity and ambient temperature. Assume the wind speed is fixed at 1 m/s.

4.1. Seawater heating system using PV/T collector

- Step 1: Assume the temperature parameters of the components at the initial time (n = 0) T^o_g, T^o_{pvl}, T^o_{ab}, T^o_t, T^o_{pw}, T^o_{ins}, T^o_{hw};
- Step 2: Put the water temperature in the PV/T collector equal to the water temperature in the seawater tank $T^o_{pw,i} = T^o_{hw}$;
- Step 3: Calculate the energy equations at the components to find the temperature T_g^{n+1}, T_{pvl}^{n+1}, T_{ab}^{n+1}, T_t^{n+1}, T_{pw}^{n+1}, T_{ins}^{n+1}, T_{hw}^{n+1} at time n+1. Calculation results will be saved into vector (V) and compared between computations using number of iterations (k).
  +If $\left|V^k - V^{k-1}\right| > 10^{-6}$ continue the iteration at k+1
  +If $\left|V^k - V^{k-1}\right| \le 10^{-6}$ results converged
- Step 4: Results in Step 3 are used to calculate the values of Q_{c1} and Q_{c2}.
  +If $\left|\dfrac{Q_{c1} - Q_{c2}}{Q_{c1}}\right| > 10^{-2}$ repeat Step 2 with $T_{pw,i} = T_{pw,i} - 0.01$
  +If $\left|\dfrac{Q_{c1} - Q_{c2}}{Q_{c1}}\right| \le 10^{-2}$ results converged
- Step 5: Output the values of temperatures T_g^{n+1}, T_{pvl}^{n+1}, T_{ab}^{n+1}, T_t^{n+1}, T_{pw}^{n+1}, T_{ins}^{n+1}, T_{hw}^{n+1} at time n+1.
- Step 6: Calculate the energy values P_{pump}^{n+1}, P_{grid}^{n+1}, η_{th}^{n+1}, η_e^{n+1}, η_{energy}^{n+1} at time n+1.
- Step 7: Take the values found in Step 5 and go back to Step 1 to find the values at the next time ($t + \Delta t$), and so on until the end.
- Step 8: Output all results
- Step 9: Stop the program

4.2. Single basin solar still

+ Day time

- Step 1: Assume the temperature parameters of the components at the initial time (n = 0) T^o_g, T^o_{sw}, T^o_b.
- Step 2: Calculate the energy equations at the components to find the temperature T_g^{n+1}, T_{sw}^{n+1}, T_b^{n+1} at time n+1. Calculation results will be saved into vector (V) and compared between computations using number of iterations (k).
  +If $\left|V^k - V^{k-1}\right| > 10^{-6}$ repeat at k+1
  +If $\left|V^k - V^{k-1}\right| \le 10^{-6}$ results converged
- Step 3: Output the temperature values T_g^{n+1}, T_{sw}^{n+1}, T_b^{n+1} at the time n+1.
- Step 4: Calculate distilled water yield m_{ev}^{n+1} at the time n+1.
- Step 5: Take the values found in Step 3 and go back to step 1 to find the values at the next time ($t + \Delta t$), and so on until the end.
- Step 6: Output all results.
- Step 7: Stop the program.

+ Nighttime

When distilling at night, because there is no longer solar radiation, at this time, the weather data included in the simulation program are only left with ambient temperature and wind speed. Using the simulation diagram for the single basin still (Fig. 7) with the initial water temperature in the distillation basin T^o_{sw} equal to the hot water temperature in the tank, the distillation results at night are achieved.

5. Results and discussion

5.1. Validating the calculating results with experimental data

To verify the simulation results, the experiment was conducted simultaneously for the water heating system using PV/T collector in daytime and the basin still during day and night. The whole system was tested from July 7th to July 22nd in Ho Chi Minh City, Vietnam. In this paper, the data of July 22nd is chosen to present. Solar radiation, ambient temperature and wind speed were measured every 5 min, as shown in Figs. 8 and 9. As shown in Fig. 8, solar radiation got maximized between 11 and 12 h at 900 (W/m²) and the ambient temperature remained around 35°C during the experiment. Fig. 9 also shows that the wind speed changes rapidly, averaging at 1.4 (m/s).

The location for mounting the temperature sensor on the PV/T collector is shown in Fig. [illegible]. The temperature sensors of the glass cover and the absorbing plate were mounted at positions 1, 2, 3, 4. Temperature sensors of water in and out of each pipe pass were mounted at positions 5, 6, 7, 8. When comparing experimental and simulation results, the temperature values of the glass cover component (T_g), absorbing plate (T_{ab}) and pure water (T_{pw}) are the average values of the sensors, correspondingly. Similarly, the inside of the hot water tank was also fitted with 3 temperature sensors to measure the water temperature at the bottom, middle and top of the tank. Experimental values of water temperature in the tank (T_{hw}) are the average value of 3 sensors and are compared with simulation. Solar radiation data (I_s), ambient temperature (T_a), wind speed (v_a) and all measured values at temperature sensors were recorded and

RETRACTED

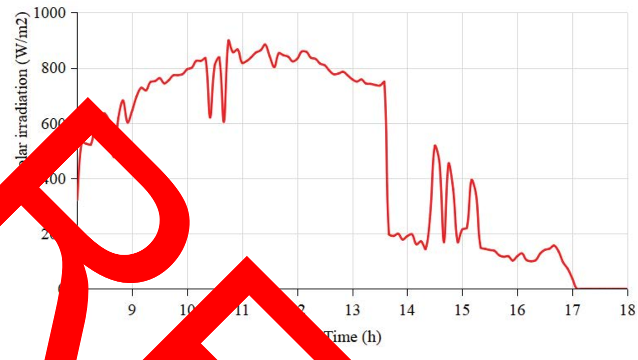

Fig. 8. Solar radiation on 22/07/2022.

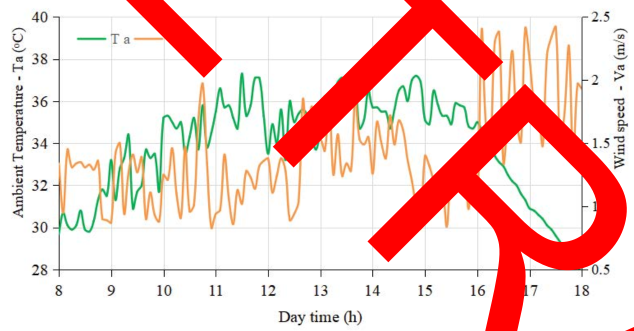

Fig. 9. Ambient temperature and wind speed on 22/07/2022.

saved automatically every 5 min. Distilled water yield was recorded every 30 min.

The error between simulation and experimental results is calculated by:

$$\overline{\text{Er}} = \frac{1}{m}\sum_{n=1}^{m}\left|\frac{Y_{\text{meas},n} - Y_{\text{pred},n}}{Y_{\text{meas},n}}\right| \times 100\ (\%) \quad (60)$$

where m is the total number of times of recording experimental values, $Y_{\text{pred},n}$ and $Y_{\text{meas},n}$ are simulated and experimental values at the nth time.

The changing in the experimental and simulation temperatures of the glass cover and seawater in the basin still during the day is shown in Fig. 10. The graph shows that the experimental and simulation curves have the same shapes. The average error between simulation and experiment of glass cover is 5.22% and that of sea water is 4.24%. The experimental line shows that the difference in temperature of the glass cover and sea water is small at the beginning due to low radiation intensity, over time the difference becomes larger, fluctuating about 10°C in the period from 12 to 13 h30. Experimental data also shows that the temperature of sea water and glass cover greatly depends on the intensity of solar radiation because the water thickness in the basin is thin, about 2 cm, so the thermal inertia is small. The temperature of water and glass cover gradually increased with the intensity of solar radiation and peaked at about 71°C and 63°C, respectively between 12h30 and

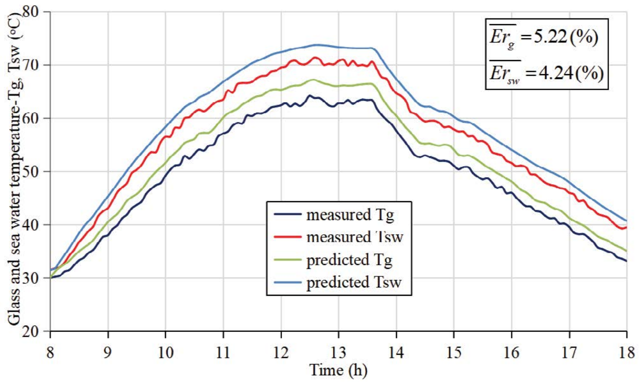

Fig. 10. Temperature change during operation of glass cover and seawater at the basin still during the day.

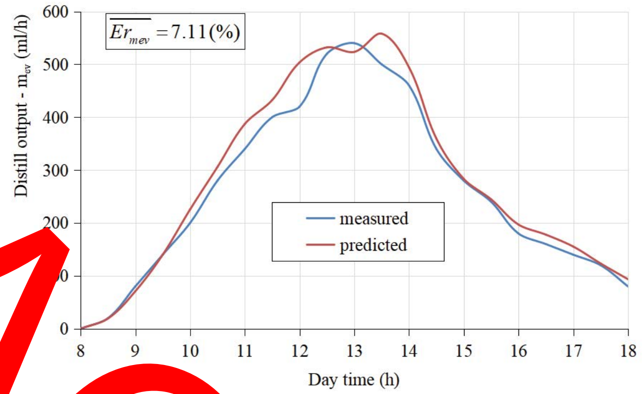

Fig. 11. Distilled water yield obtained during daytime operation.

13h30, then dropped suddenly before gradually decreasing and reaching 39.5°C and 33.2°C respectively at 18 h.

Distilled water production during the day by experiment and simulation is shown in Fig. 11. The graph shows that the simulation and experimental lines have the same trend of increasing and decreasing but the error is small in the early period from 8 am to 10 am and the next period from 14h20 to 18 h. The error increases gradually from 10 am and is most obvious at 13h, about 20%. Total experimental distilled water production reached 2.72 L while simulation reached 2.91 L, so the error between simulation and experiment is 7.11%.

Fig. 12 shows the change in temperature of the water in the tank over time between simulation and experiment. The graph shows that the predicted results of the simulation program are quite accurate compared to the experiment in most of the time, the average error is 4.3[illegible] Looking at the experimental line on the chart, Fig. 12 shows that the water temperature gradually increased and peaked 51.5°C at 13h55, then decreased slightly and reached 48.7°C at 16 h.

Fig. 13 shows that the ambient temperature decreases with time and the wind speed changes continuously during the experimental time. From 18:00 to 19:00, all seawater used for daytime which left over in the basin was discharged out and the seawater in the heat exchange tank

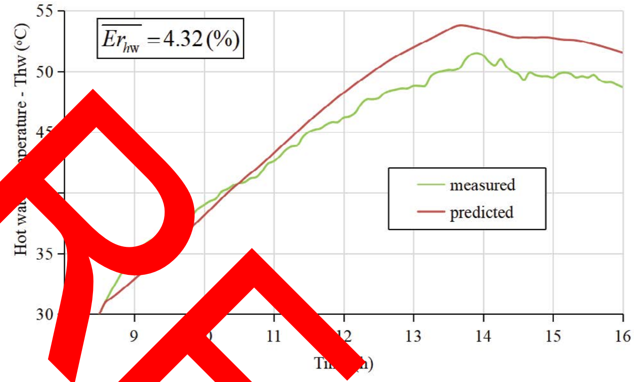

Fig. 12. Sea water temperature in the hot water tank.

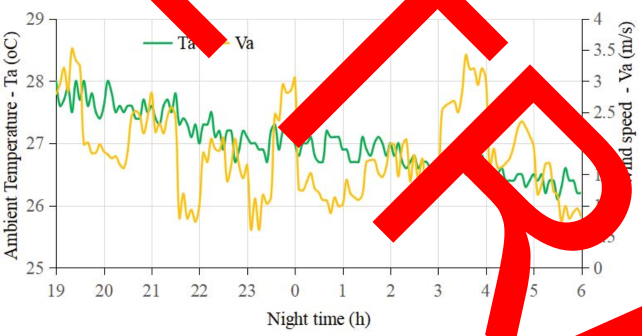

Fig. 13. Ambient temperature and wind speed in the evening of 22nd and morning of July 23rd, 2022.

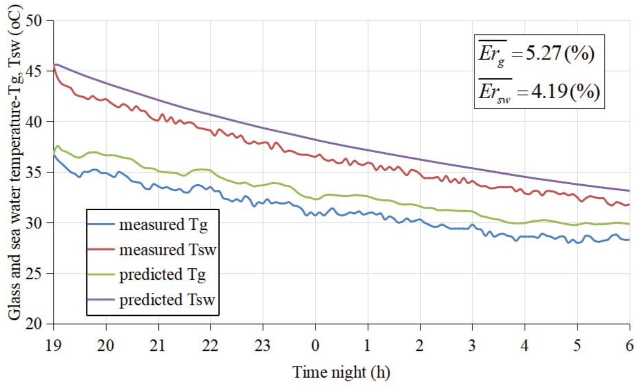

Fig. 14. Temperature changing during operation of glass cover and seawater at the basin still at night.

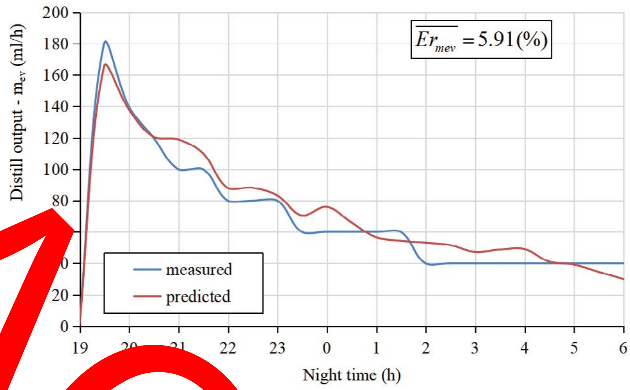

Fig. 15. Distilled water yield obtained during night operation.

would be filled in the still. Due to the heat loss when storing in the tank and the loss when filling, the sea water temperature when down to 45.6°C.

After the period from 16 h to 19 h, due to heat loss to the environment, 100 L of water in the tank decreased from 48.7°C to 45.6°C. Fig. 14 shows the experimental and simulation temperature changes of the glass cover and sea water at night. The verification results show that the average error between simulation and experiment of the glass cover is 5.27% and that of sea water is 4.19%. Experimental data shows that the temperature of the glass cover and sea water decreases steadily over time, the temperature of water and glass cover reaches 31.8°C and 28.3°C, respectively at 6h. As shown in Fig. 13, the glass cover temperature at 6 h is about 2°C higher than the ambient temperature, which shows that the system's ability to distill water at night is very high, lasting for 11 h.

Fig. 15 depicts the simulation and experimental distillate yield at night. The graph shows that the results between simulation and experiment are quite similar. The total production of distilled water in simulation is 770 mL while experimental is 815 mL, so the error between simulation and experiment is 5.91%. Because there is no influence by the intensity of solar radiation, the error in distilled water yield between simulation and experiment at night is smaller than that during the day.

As discussed above, Figs. 10–15 show that there are good agreements between simulation and experimental results. The next step, this simulation program is used to make recommendations on the optimal volume of water in the tank and thereby predict the production of distilled water at typical days of months from January to June.

5.2. Optimizing the volume of water in the tank

Using data of solar irradiance and ambient temperature of typical days for 6 months from January to June (Fig. 16), the written simulation was used to calculate the energy efficiency with G_{pw} flows varying from 0.01 to 0.05 kg/s. From the calculation results, the energy efficiency values were averaged and got the results as shown in Fig. 17. The results show that the PV/T collector water heating system has the highest average energy efficiency with G_{pw} = 0.02 kg/s. Fig. 17 also shows that the larger the volume of hot water in the tank, the higher the energy efficiency. This can be explained because the larger the volume of water in the tank, the smaller the temperature of the cooler entering the collector, the greater the ability to receive heat, so the thermal and electrical efficiency increases, leading to increased energy efficiency.

Using a flow rate of G_{pw} = 0.02 kg/s, the simulation program determined the distilled water output for hot water volumes in the tank from 50 to 150 L for typical days of the month. The results as described in Fig. 18 show that the system achieves the largest distilled water output in January,

RETRACTED

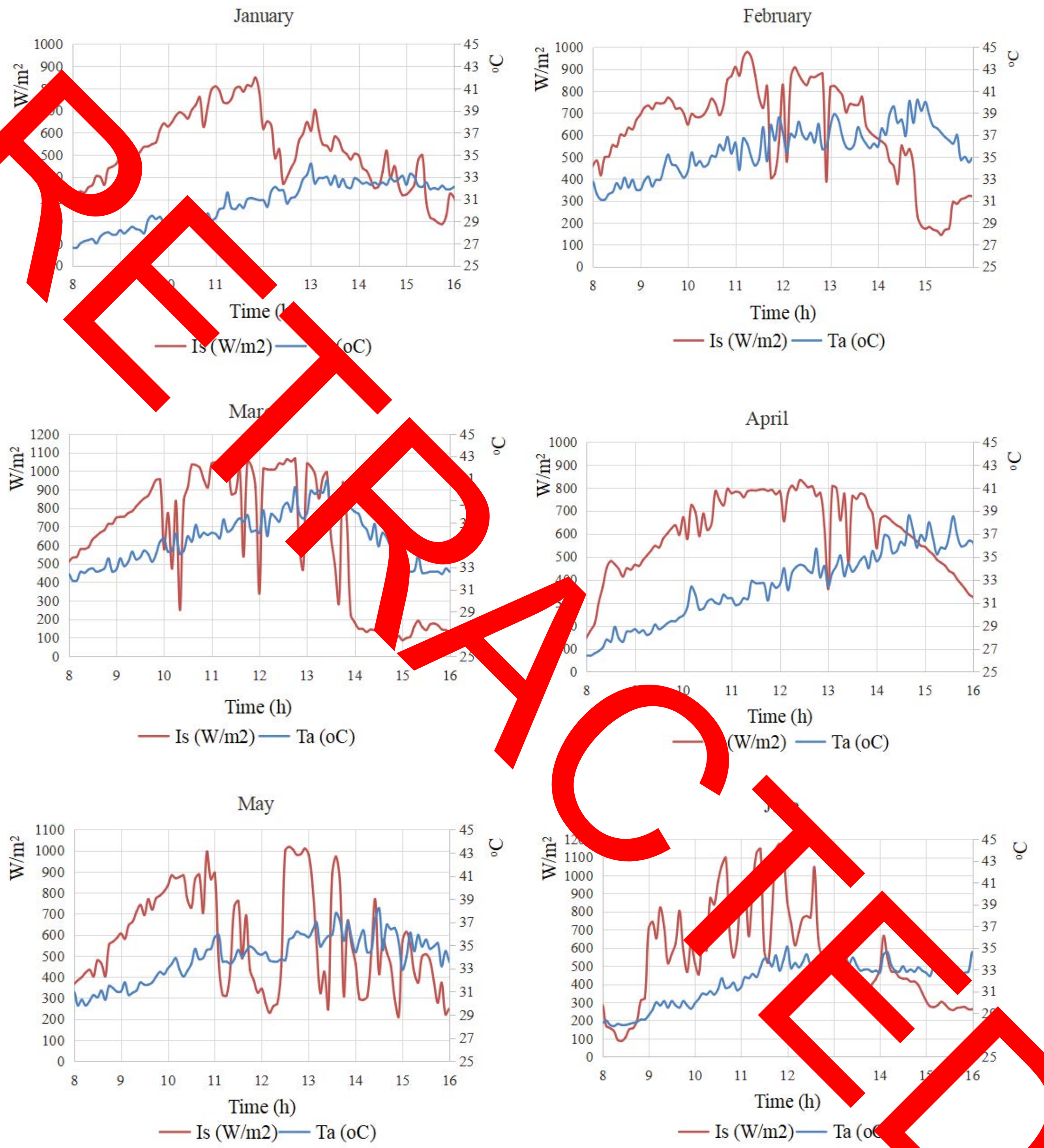

Fig. 16. Solar radiation intensity and ambient temperature of typical days of the months.

March, April, and June when the volume of hot water in the tank is at 100 L. In February the optimal volume is 80 L while in May it is 110 L.

Under the weather conditions in April and water flow G_{pw} = 0.02 kg/s, the study investigated the temperature change over time of the components in the PV/T collector (glass cover (T_g), PV layer (T_{pvl}), absorber (T_{ab}), tube (T_t)) and hot water in the tank (T_{hw}) when changing the tank volume for 4 levels at 60, 80, 100 and 120 L, respectively. The results are shown in the four graphs of Fig. 19. In general, the lower the tank volume, the higher the temperature of the components in the PV/T collector and the hot water. Besides, there is little temperature difference between glass cover, PV layer, absorber and

RETRACTED

tube because these components are linked together as a whole. As the radiation intensity is higher and the hot water temperature is greater, the difference in temperature between these components becomes more obvious. Fig. 1[illegible]o illustrates that, in all 4 volume levels of the tan[illegible]hen the hot water is heated to the peak temperat[illegible], there w[illegible] be a tendency to reverse heat transfer to [illegible]/T colle[illegible]r components and loss to the environment [illegible] to h[illegible] transfer. Then the hot water temperature will d[illegible]

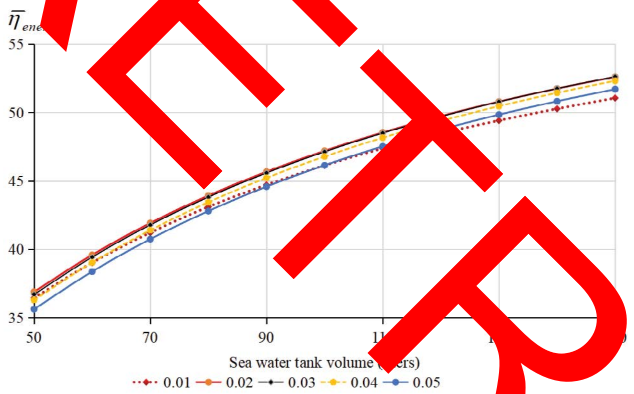

Fig. 17. Average energy efficiency of water heatin[illegible]stem using PV/T collector.

5.3. Distilled water production prediction

From the above optimal results of the G_f flow and optimal tank volume findings, the simulations were done to predict the daytime and nighttime distillate production of typical days in the months. The results in Fig. 20 show that total distillate production during the day and night in March is the highest, with 3.76 L/d, followed by February, April, May, June and May with 3.58, 3.36, 3.13, 2.81 and 2.5 L/d respectively. Fig. 20 also shows that the nocturnal

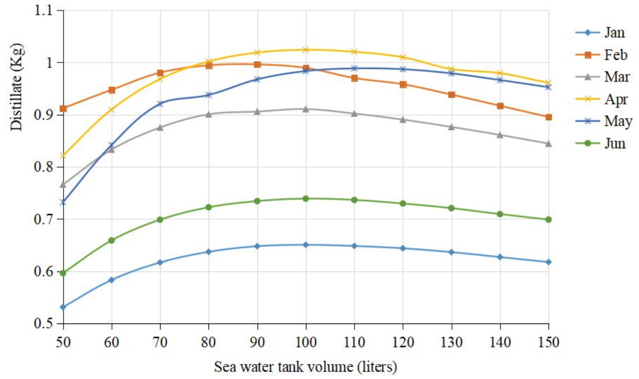

[illegible] Distilled water output at night in months corresponding to t[illegible] volume of water in the tank.

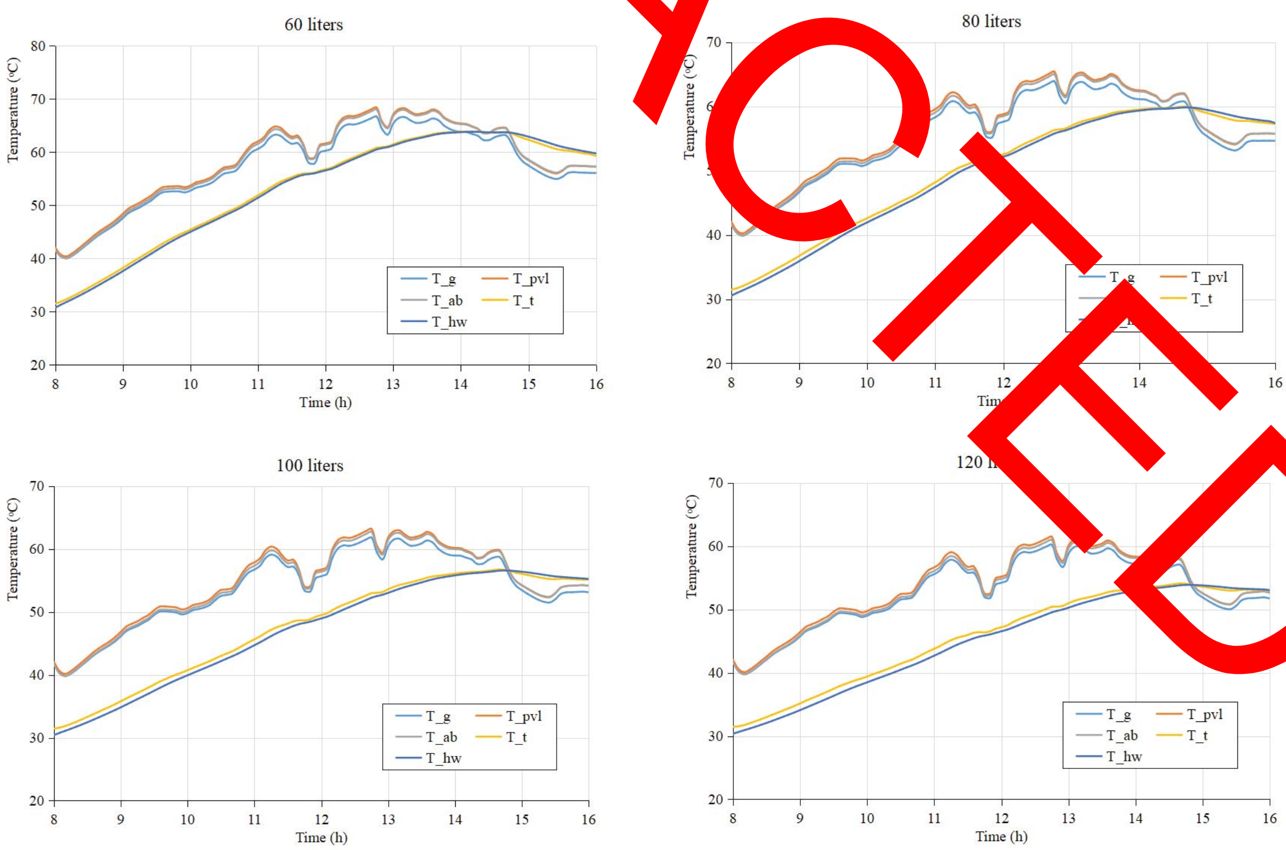

Fig. 19. Temperature of components over time as the tank volume changes.

RETRACTED

Fig. 20. Distilled water production during day and night.

distillation potential of the system is huge as the distillation output at night ranges from [illegible].1% to 29.4% of the total distilled water production. Especially through the chart, it is also seen that the use hot water produced from PV/T collector to distill water at night increases the output of distilled water from 35.2% to 41.7%. This has enormous implications for water distillation potential.

6. Conclusions

This paper introduced a new idea of PV/T system, in which the water used to cool solar cells (PV cells) is used to provide hot water at night for a solar passive single basin still – a distillation device with simple design and operation. This proposed PV/T system helped the solar still produce distilled water at both day and night, hence increasing the distilled yield in comparison with that of conventional solar still. The article also presented a simulation program written in MATLAB based on the thermal analysis equations of PV/T system equipment, thereby calculating the parameters of the equipment as well as the power output and distilled water of the whole PV/T system. The comparison of the calculated results and the experimental results showed that the written simulation program has high accuracy and reliability. The errors between experimental and simulation results were around 4.24% to 7.11%. Then, the simulation program was used to recommend the optimal volume of water in the tank and thereby predicted the production of distilled water at typical days of 6 months from January to June. The simulation results showed that the use of hot water from PV/T collector to distill water at night increased the output of distilled water from 35.2% to 41.7% compared to that of traditional solar single basin stills.

In the next studies, the feasibility of applying hot water supply systems using PV/T collectors for water distillation systems other than single basin solar still will be conducted and evaluated. This future work will hopefully contribute to solve two urgent problems of electricity shortage and improving freshwater sources, helping to improve lives for people in remote areas, rurals and islands.

Symbols

h	—	Heat transfer coefficient, W/m²·K
h_c	—	Convective heat transfer coefficient, W/m²·K
h_r	—	Radiative heat transfer coefficient, W/m²·K
h_e	—	Evaporative heat transfer coefficient, W/m²·K
k	—	Thermal conductivity, W/m·K
Q	—	Energy rate, W
M	—	Mass, kg
m_{ev}	—	Distillate output, kg/s
A	—	Surface area, m²
v_a	—	Air velocity, m/s
c_p	—	Specific heat capacity, J/kg·K
T	—	Temperature, K
D	—	Diameter, m²
Pe	—	Perimeter, m
H	—	Height, m
L	—	Length, m
p	—	Pressure, Pa
P	—	Electrical power, W
E	—	Specific electrical power, W/m²
f	—	Packing factor
Re	—	Reynolds number
Nu	—	Nusselt number
I_s	—	Solar radiation intensity, W/m²
G	—	Mass flow rate, kg/s
h_{fg}	—	Latent heat of vaporization of water, J/kg·K
t	—	Time, s
Δp	—	Pressure drop, Pa

Greek

α	—	Absorptivity
τ	—	Transmittance
σ	—	Stefan–Boltzmann constant, 5.67×10^{-8}, W/m²·K⁴
ρ	—	Density, kg/m³
ω	—	Water velocity, m/s
ε	—	Emissivity
δ	—	Thickness, m
η	—	Efficiency
μ	—	Dynamic viscosity, Pa·s

Subscripts

g	—	Glass
pw	—	Pure water
sw	—	Sea water
hw	—	Hot sea water in tank
a	—	Ambient
ab	—	Absorber
pvc	—	Photovoltaic cell
PV/T	—	Photovoltaic/thermal collector
pvl	—	PV layer
t	—	Tube
b	—	Basin liner
c	—	Convection, coil, critical
r	—	Radiation, reference
e	—	Evaporation
ins	—	Insulation
grid	—	On grid
th	—	Thermal

e, elec	—	Electrical
i	—	In
o	—	Out
ad	—	Thermal adhesive
v	—	Vapor
inv	—	Inverter
β	—	Solar cell temperature coefficient

References

[1] N.T. Bao, The Mathematical Model of Basin-Type Solar Distillation Systems, V. Steffen, Ed., Distillation – Modelling, Simulation and Optimization, InTechOpen, 2019, DOI: 10.5772/intechopen.[illegible]

[2] N.T. Bao, Textbook on Renewable Energy and Sustainable Development, Vietnam National University Publishing House, 2021.

[3] A. Akbarzadeh, T. Wadowski, Heat-pipe-based cooling systems for photovoltaic cells under concentrated solar radiation, Appl. Therm. Eng., 16 (1996) 81–87.

[4] E. Chaniotakis, Modelling and Analysis of Water Cooled Photovoltaics, M.Sc. Thesis, Department of Mechanical Engineering, University of Strathclyde, Glasgow, Scotland, 2001.

[5] H. Batoul, Flow Simulation Improves Photovoltaic Solar Panel Performance, Technical Report, Schueco International, Paris, France, 2008.

[6] J.K. Tonui, Y. Tripanagnostopoulos, Improved PV/T solar collectors with heat extraction by forced or natural air circulation, Renewable Energy, 32 (2007) 623–637.

[7] D.H. Ho, A.T. Truong, T.B. Nguyen, Design a cooling system for solar cells to increase PV output, Vietnam Mech. Eng. J., 291 (2022) 25–34 (in Vietnamese).

[8] E. Hedayati-Mehdiabadi, F. Sarhaddi, F. Sobhnamayan, Energy analysis of a stepped cascade solar still connected to photovoltaic thermal collector, Int. J. Automot. Mech. Eng., 14 (2017) 4805–4825.

[9] J.A. Duffie, W.A. Beckman, Solar Engineering of Thermal Processes, John Wiley & Sons, Inc., 1990.

[10] S. Bhattarai, J.-H. Oh, S.-H. Euh, G.K. Kafle, D.H. Kim, Simulation and model validation of sheet and tube type photovoltaic thermal solar system and conventional solar collecting system in transient states, Sol. Energy Mater. Sol. Cells, 103 (2012) 184–193.

[11] A. Bejan, Heat Transfer, New York, Wiley, 1993.

[12] X.X. Zhang, X.D. Zhao, J.C. Shen, J.H. Xu, X.T. Yu, Dynamic performance of a novel solar photovoltaic/loop-heat-pipe heat pump system, Appl. Energy, 114 (2014) 335–352.

[13] E. Bellos, C. Tzivanidis, Multi-objective optimization of a solar assisted heat pump-driven by hybrid PV, Appl. Therm. Eng., 149 (2019) 528–535.

RETRACTED